A. I. Casian[1], J. Pflaum[2], I. I. Sanduleac[1]

[1]Technical University of Moldova, MD-2004, Chisinau, Rep. of Moldova
[2]Julius-Maximilians University, Am Hubland, 97074 Wurzburg, Germany

PROSPECTS OF LOW DIMENSIONAL ORGANIC MATERIALS FOR THERMOELECTRIC APPLICATIONS

The aim of the paper is to present briefly the state-of-art and to analyze the prospects of thermoelectricity based on organic materials. It is shown that low dimensional nanostructured organic crystals have the highest prospects for thermoelectric applications. In these crystals, the density of electronic states is increased due to the low dimensionality of carrier spectrum and the interdependence between electrical conductivity, thermopower and the electronic thermal conductivity is somewhat overcome due to more diverse internal interactions. The thermoelectric properties of tetrathiotetracene–iodide crystals, TTT_2I_3 are analyzed in the frame of a more complete 3D physical model and the optimal parameters are determined in order to achieve values of the thermoelectric figure of merit at room temperature of ZT ~ 2 and even higher.

Key words: organic crystal, tetrathiotetracene–iodide crystal, 3D physical model, electrical conductivity, thermopower, electronic thermal conductivity, thermoelectric figure of merit.

Introduction

The search and investigation of new materials with increased thermoelectric figure of merit, *ZT*, continue to be an important and actual problem of solid state physics. In this domain during the last decade impressive results have been obtained. A value of $ZT \sim 2.2$ at 800 K was reported [1] in complex chalcogenide compounds of the type $AgPb_mSbTe_{2+m}$. $ZT \sim 2.4$ has been measured [2] at room temperature in *p*-type Bi_2Te_3/Sb_2Te_3 superlattice structures. Harman [3] has obtained $ZT \sim 3$ in *PbTeSe* quantum dot superlattices [3], and even $ZT \sim 3.5$ [4, 5]. It is known that for $ZT > 3$ the thermoelectric generators and refrigerators become economically competitive with those that are usually used nowadays. But the thermoelectric devices have evident advantages: no mechanical wear, long life, high reliability, no environmental pollution, noiseless operation. Therefore, the obtaining of materials with $ZT > 3$ is a big progress in this area. However, in spite of these impressive results, there are many difficulties for their practical applications, because the technology to obtain such structures is complicated, expensive and can not be applied for large scale production. Now the used thermoelectric materials have still low efficiency. Therefore, the commercialization of thermoelectric devices has still limited applications. Nevertheless, mass production of miniaturized thermoelectric modules has succeeded to maintain constant temperatures in the operation of laser diodes [5], seat heatings fabricated by Gentherm Corporation and installed in hundreds of thousands of vehicles each year [6, 7], portable beverage coolers [8] and other applications.

In the last years organic compounds attract more and more attention as materials which are less expensive, have more diverse and often unusual properties in comparison with their inorganic counterparts and their molecular structure can be easily modified to tune the desirable physical and chemical properties. Besides, the organic materials usually have low thermal conductivity due to their mainly dispersive interaction.

In poly3,4-ethylenedioxythiophene (PEDOT) doped by polystyrenesulphonate (PSS) thin films of *p*-type conductivity a value of the thermoelectric figure of merit $ZT = 0.42$ at room temperature has been measured [9] by optimizing the carrier concentration. It is reported also a value of $ZT = 1.02$ in PP-PEDOT/TOS [10] films, but the value of the thermal conductivity is taken from another study and thus has not been confirmed for the reported films of higher electrical conductivity. For *n*-type materials the best result is obtained in powder-processed inorganic hybrid polymer, poly[Kx-(*Ni*-ett)], with a $ZT = 0.2$ at 400 K [11].

It is expected that the nanocomposites of organic and inorganic components may have an even better thermoelectric performance than their individual components [12-16]. But no significant improvement in the figure of merit of this material class has been achieved until now. In PEDOT-based nanocomposites *ZT* varies between 0.02 and 0.1 [17]. The highest value of $ZT = 0.57$ at room temperature was measured in phenyl acetylene-capped silicon nano particles [18].

Different theoretical models describing the thermoelectric transport in organic materials have been also developed [19-24]. Ref. [24] should be mentioned explicitly, because a value of $ZT \sim 15$ at room temperature has been predicted in molecular nanowires of conducting polymers in spite of hopping conducting mechanism that usually leads to smaller carrier mobilities than band transport.

In highly conducting quasi-one dimensional (Q1D) organic charge transfer crystals we have predicted even higher values of $ZT \sim 20$ under some conditions [25, 26]. However, all predictions were made on the base of a strictly one dimensional physical model. In existing Q1D crystals of tetrathiotetracene-iodide, TTT_2I_3, grown from solution [27] with measured electrical conductivity $\sigma_{xx} = 1.8 \cdot 10^5\ \Omega^{-1}m^{-1}$, Seebeck coefficient $S_{xx} = 39\ \mu V/K$ and thermal conductivity $\kappa_{xx} = 1.0\ Wm^{-1}K^{-1}$ along the conductive chains only $ZT \cong 0.1$ was obtained at room temperature [28]. Such low value of *ZT* is explained by the fact that the crystals were not very pure and the parameters were not optimized.

More detailed modelings of the thermoelectric properties of TTT_2I_3 crystals, taking into account the interchain interaction in 2D approximation were also presented [29-31]. It was shown that in not very perfect crystals the results obtained by 2D and 1D approximation are very similar. First theoretical calculations in a more comprehensive 3D physical model have been partially realized in [32] and [33].

The aim of this paper is to present detailed modeling of the thermoelectric properties in the most complete 3D physical model and to determine realistic values of the thermoelectric figure of merit in TTT_2I_3 crystals with enhanced degree of purity. The criteria, when the simpler 1D model can be applied will be elucidated.

Three-dimensional crystal model for TTT_2I_3

From the structural point of view the Q1D crystals of tetrathiotetracene-iodide, TTT_2I_3, are formed from segregate stacks or chains of *TTT* molecules and iodine [30]. However, only *TTT* chains are conductive due to considerable overlap of π – electron wave functions along their stacking direction. Two molecules of *TTT* supply one electron to the iodine chain formed from I_3^- ions which play the role of acceptors. The electrons on I_3^- ions are in a rather localized states and do not participate in the transport. Thus, the carriers are holes. The electrical conductivity along *TTT* chains is almost of three orders of magnitude bigger than in transversal directions. Previously, due to this property the simpler 1D physical model was used [34-36] and the crystal was considered to be formed from independent 1D chains packed into a 3D crystalline structure. However, in reality some

additional interaction between the 1D conductive chains exists. Of course, this interchain interaction will affect somehow the results of the 1D approximation, especially in crystals with high degree of purity, when this interaction will limit the carrier mobility. Therefore, it is very important to determine the effect of interchain interaction on the thermoelectric properties in real crystals and, in this regard, to determine the criteria, when the simpler 1D model is still valid.

The charge and energy transport are described in the tight binding and nearest neighbors approximations. In the 3D model the energy of the hole with the quasi-wave vector $\boldsymbol{k}$ and its orthogonal projections (k_x, k_y, k_z), measured from the top of conduction band, has the form

$$E(\boldsymbol{k}) = -2w_1(1-\cos k_x b) - 2w_2(1-\cos k_y a) - 2w_3(1-\cos k_z c), \tag{1}$$

where w_1, w_2, w_3 are the hole transfer energies from a given molecule to the nearest ones along lattice vectors $\boldsymbol{b}$, $\boldsymbol{a}$, $\boldsymbol{c}$, the axes x, y, z are directed along $\boldsymbol{b}$, $\boldsymbol{a}$, $\boldsymbol{c}$, the conductive chains are directed along $\boldsymbol{b}$, therefore it is considered that w_1 is much bigger than w_2 and w_3.

Only longitudinal acoustic phonons are taken into consideration with the dispersion law

$$\omega_{\boldsymbol{q}}^2 = \omega_1^2 \sin^2(bq_x/2) + \omega_2^2 \sin(aq_y/2) + \omega_3^2 \sin(cq_z/2), \tag{2}$$

where the quasi-wave vector $\boldsymbol{q}$ has the projections (q_x, q_y, q_z), and ω_1, ω_2 and ω_3 are the limit frequencies in the x, y and z directions. Due to the quasi-one-dimensionality ω_1 is much bigger than ω_2 and ω_3.

As in previous 1D and 2D cases, two of the most important interactions of holes with acoustic phonons are considered, generalized for the 3D case. One interaction is similar to that of deformation potential with three coupling constants w_1', w_2' and w_3' determined by the variation of transfer energies with respect to intermolecular distances. The second interaction is similar to that of a polaron and is caused by the induced polarization of molecules surrounding the conduction hole. The coupling constant of this interaction is determined by the mean polarization of the molecules α_0.

The square of matrix element module describing the hole-phonon interaction has the form

$$\left|\mathrm{A}(\boldsymbol{k},\boldsymbol{q})\right|^2 = 2\hbar/(MN\omega_q)\{w_1'^2[\sin(k_x b) - \sin((k_x - q_x)b) + \gamma_1 \sin(q_x b)]^2 +$$

$$+ w_2'^2[\sin(k_y a) - \sin((k_y - q_y)a) + \gamma_2 \sin(q_y a)]^2 + w_3'^2[\sin(k_y c) - \sin((k_y - q_y)c) + \gamma_3 \sin(q_y c)]^2\}. \tag{3}$$

Here M is the mass of *TTT* molecule, N is the number of molecules in the basic region of the crystal. The parameters γ_1, γ_2 and γ_3 have the meanings of amplitudes ratios between the second interaction and the first one along the chains and in transversal directions

$$\gamma_1 = 2e^2\alpha_0/(b^5 w_1'), \quad \gamma_2 = 2e^2\alpha_0/(a^5 w_2'), \quad \gamma_3 = 2e^2\alpha_0/(c^5 w_3'), \tag{4}$$

where e is the elementary charge.

The scattering of holes by impurities is considered as point like and neutral is also taken into account. The impurity scattering rate is described in this case by a dimensionless parameter D_0 which is proportional to the impurity concentration and can be assumed very small, if the crystal purity is rather high. The variation of wave vectors $\boldsymbol{k}$ and $\boldsymbol{q}$ is considered in the whole Brillouin zones for holes and phonons, because the conduction band is not very large and the Debye temperature is relatively low for organic materials.

Transport properties

Let a weak electrical field and a weak temperature gradient be applied along the conductive chains. At room temperature it is possible to neglect the phonon energy and the transversal kinetic energy of the hole in the scattering processes, because they are much smaller than the kinetic energy of the hole along the chains. Then, the linearized kinetic equation is solved analytically and the electrical conductivity σ_{xx}, the Seebeck coefficient S_{xx}, the electronic thermal conductivity κ^e_{xx} and $(ZT)_{xx}$ can be expressed through the transport integrals R_n as follows

$$\sigma_{xx} = \sigma_0 R_0,\ S_{xx} = (k_0 / e)(2w_1 / k_0 T) R_1 / R_0, \tag{5}$$

$$\kappa^e_{xx} = [4w_1^2 \sigma_0 / (e^2 T)](R_2 - R_1^2 / R_0),\ (ZT)_{xx} = \sigma_{xx} S_{xx}^2 T / (\kappa^L_{xx} + \kappa^e_{xx}), \tag{6}$$

where

$$\sigma_0 = (2e^2 M v_{s1}^2 w_1^3 r) / (\pi^2 \hbar abc (k_0 T)^2 w_1'^2), \tag{7}$$

With $r = 4$ being the number of molecular chains contained in the transversal section of the elementary cell, k^L_{xx} is the lattice thermal conductivity, v_{s1} is the velocity of sound along the chains and R_n are the transport integrals

$$R_n = \int_0^2 d\varepsilon \int_0^{\pi} d\eta \int_0^{\pi} d\varsigma \varepsilon (2-\varepsilon) n_{\varepsilon,\eta,\varsigma} (1 - n_{\varepsilon,\eta,\varsigma}) \times$$

$$\times \frac{[\varepsilon + d_1(1-\cos\eta) + d_2(1-\cos\varsigma) - (1+d_1+d_2)\varepsilon_F]^n}{\gamma_1^2(\varepsilon-\varepsilon_0)^2 + D_0 + \{d_1^2(1+\gamma_2^2+2\sin^2\eta - 2\gamma_2\cos\eta) + d_2^2(1+\gamma_3^2+2\sin^2\varsigma - 2\gamma_3\cos\varsigma)\}/(8\varepsilon(2-\varepsilon))}. \tag{8}$$

Here, in order to compare with the 1D model, new dimensionless variables $\varepsilon = (1-\cos(k_x b))$, $\eta = k_y a$ and $\varsigma = k_z c$ were introduced, $n_{\varepsilon,\eta,\varsigma}$ is the Fermi distribution function in this new set of variables, $\varepsilon_0 = (\gamma_1 - 1)/\gamma_1$ is the dimensionless resonance energy in the relaxation time in units of $2w_1$, $d_1 = w_2/w_1 = w_2'/w_1'$, $d_2 = w_3/w_1 = w_3'/w_1'$, $\varepsilon_F = E_F/2w_1$ is the 1D Fermi energy in units of $2w_1$. The 3D Fermi energy will be $2w_1(1+d_1+d_2)\varepsilon_F$. The parameter D_0 describes the hole scattering by impurities

$$D_0 = n_{im}^{3D} I^2 V_0^2 \frac{M v_s^2}{4b^3 a c w_1'^2 k_0 T}, \tag{9}$$

where n_{im}^{3D} is the density of impurities, I is the height of impurity potential and V_0 is the domain of potential action.

If we put in (8) $d_1 = 0$ and $d_2 = 0$, the integrals for η and ς can be calculated analytically and the results of the previously discussed 1D model are obtained. It can be seen that in this case the expression in the integral in (8) has a maximum for ε close to ε_0 and this maximum can be rather high, if D_0 is sufficiently small. It is a consequence of mutual compensation of the two mentioned hole-phonon interactions for states in the conduction band close to ε_0. In the 1D case this maximum is limited by D_0. Now the maximum is limited also by the rate of interchain scattering. Therefore, it becomes important to determine the criteria, when the entertain scattering will predominate, and further crystal purification will not yield better results.

In order to determine the parameters d_1 and d_2 we have calculated the electrical conductivity in the transversal directions σ_{yy} and σ_{zz}. Along these directions the overlap of hole wave functions is very weak and it is more convenient to write the Hamiltonian of the system in the representation of localized states at *TTT* molecules. Respectively, for the *y* and *z* direction the most important term in

the Hamiltonian becomes the hole-phonon interaction and the term which describes the motion of holes in the periodic lattice potential is considered as small perturbation. Therefore, a canonical transformation is applied to the Hamiltonian which permits to take into consideration the main part of the hole-phonon interaction already in the zero approximation. This also leads to considerable narrowing of the initial conduction band along the conductive chains. As a consequence, in the transversal directions the transport becomes of hopping type and the carriers can be described as small polarons.

Expressions for σ_{yy} and σ_{zz} were calculated numerically. By comparing them with the experimental data of $\sigma_{yy} \sim \sigma_{zz} = 3.3\ \Omega^{-1}\text{cm}^{-1}$, it can be estimated that $w_2 = w_3 = 0.015 w_1$. These values are of the same order because the lattice constants *a* and *c* in *y* and *z* direction are very close to each other.

Results and discussion

Expressions (5)–(8) have been calculated numerically for quasi-one-dimensional organic crystals of TTT_2I_3 with different degrees of purity. The crystal parameters are: $M = 6.5\cdot10^5 m_e$ (m_e is the mass of the free electron), a =18.35 Å, b = 4.96 Å, c = 18.46 Å, $v_{s1} = 1.5\cdot10^3$ m/s, w_1 = 0.16 eV, w_1' =0.26 eVÅ^{-1}, r = 4, $d_1 = d_2 = 0.015$, k_{xx}^L = 0.6 WK^{-1}m^{-1}. The mean polarizability of *TTT* molecules was taken as in [30] $\alpha_0 = 45$ Å^{-3} and this leads to $\gamma_1 = 1.7$. The parameters γ_2 and γ_3 were calculated after (4). For the parameter D_0 the following values were chosen: 0.1 which corresponds to crystals grown by gas phase method [37] with stoichiometric electrical conductivity $\sigma_{xx} \sim 10^6\ \Omega^{-1}\text{m}^{-1}$; 0.02 which correspond to purer crystals grown also by gas phase method with somewhat higher $\sigma_{xx} \sim 3\cdot10^6\ \Omega^{-1}\text{m}^{-1}$, and 0.005 which corresponds to even more perfect crystals with $\sigma_{xx} \sim 6.6\cdot10^6\ \Omega^{-1}\text{m}^{-1}$ not obtained yet.

In Fig. 1 the dependences of electrical conductivity along chains σ_{xx} as functions of dimensionless Fermi energy ε_F in units of $2w_1$ are presented for these values of D_0.

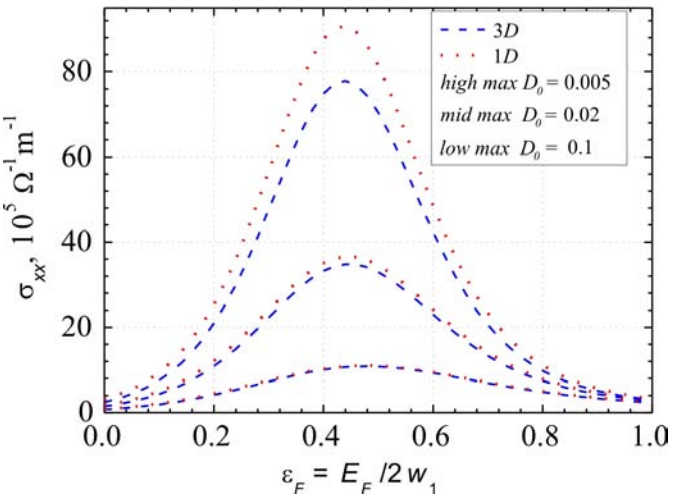

Fig.1. Electrical conductivity σ_{xx} along chains as a function of E_F for $\gamma_1 = 1.7$.

It can be seen that for not very pure crystals which corresponds to $D_0 = 0.1$ the results of the 3D model coincide with those of simpler 1D model in the entire region of ε_F variation. Even for purer crystals, i.e. $D_0 = 0.02$ the deviation of 3D model from the 1D model is still negligible. In these cases

the carrier mobility is limited by scattering at impurities, the scattering on adjacent chains does not give important contribution to σ_{xx} and the simpler 1D model may be used instead. In case of the purest crystals with stoichiometric electrical conductivity $\sigma_{xx} \sim 6.6 \cdot 10^6$ $\Omega^{-1}m^{-1}$ the deviation between 3D model and 1D amounts to ~ 18%. Now the carriers' scattering on adjacent chains gives significant contribution to σ_{xx} and the 3D model must be used.

In Fig. 2 the dependences of thermopower (Seebeck coefficient) along chains S_{xx} on Fermi energy at room temperature are presented. It is seen that the results of the models for 3D and 1D are very close across the whole interval of ε_F variation.

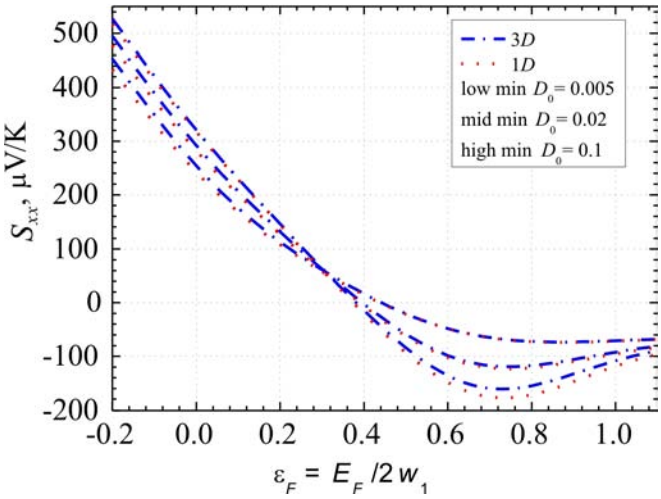

Fig. 2. Thermopower S_{xx} along chains as a function of E_F for $\gamma_1 = 1.7$.

As it is seen from (5), S_{xx} is proportional to the ratio of transport integrals R_1/R_0 and therefore is less sensitive to the interchain interaction. For stoichiometric crystals ($\varepsilon_F \sim 0.35$) S_{xx} weakly depends on crystal perfection and takes values between 35 and 40 μV/K as it is observed experimentally. With the decrease of ε_F from the stoichiometric value, S_{xx} grows considerably that is favorable for the improvement of the thermoelectric properties.

In Fig.3 the dependences of the electronic thermal conductivity along chains κ^e_{xx} on Fermi energy at room temperature are presented. It is seen that for crystals to which it corresponds $D_0 = 0.1$ and 0.02 with stoichiometric electrical conductivity $\sigma_{xx} \sim 10^6$ $\Omega^{-1}m^{-1}$ and $\sigma_{xx} \sim 3 \cdot 10^6$ $\Omega^{-1}m^{-1}$, respectively, predictions by the 3D and 1D model practically coincide. Only in the case of the purest crystals when $D_0 = 0.005$ a diminution of κ^e_{xx} by about 5% with respect to the 1D model is observed, less than in the case of σ_{xx}, where the diminution was ~ 18%. But the contribution of κ^e_{xx} to the total thermal conductivity has increased considerably. Even in less pure stoichiometric crystals κ^e_{xx} is 5.5 times bigger than κ^L_{xx} and up to 20 times in the most perfect crystals. This means that practically all thermal conductivity relates to the electronic part. It is also seen that the maxima of κ^e_{xx} are displaced to higher values of ε_F with respect to the maxima of σ_{xx}. This ensures a decrease of the Lorenz number in the interval of ε_F which is important for the increase of the thermoelectric figure of merit *ZT* and thus is favorable for the improvement of the thermoelectric properties.

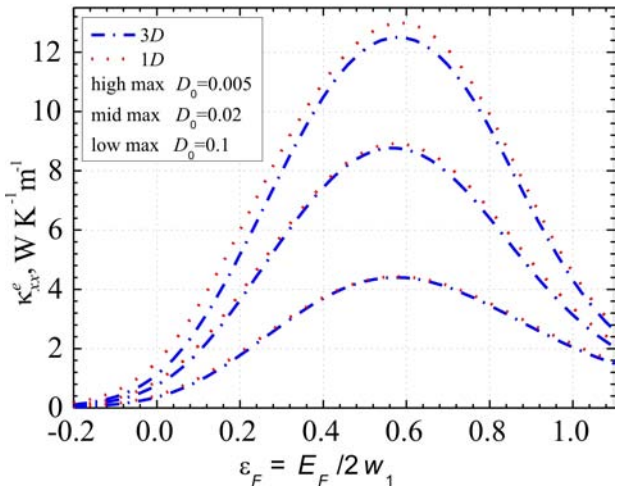

Fig.3. Electronic thermal conductivity along chains κ^e_{xx} as a function of E_F for $\gamma_1 = 1.7$.

The dependences of the thermoelectric figure of merit along chains *ZT* on Fermi energy at room temperature are presented in Fig.4.

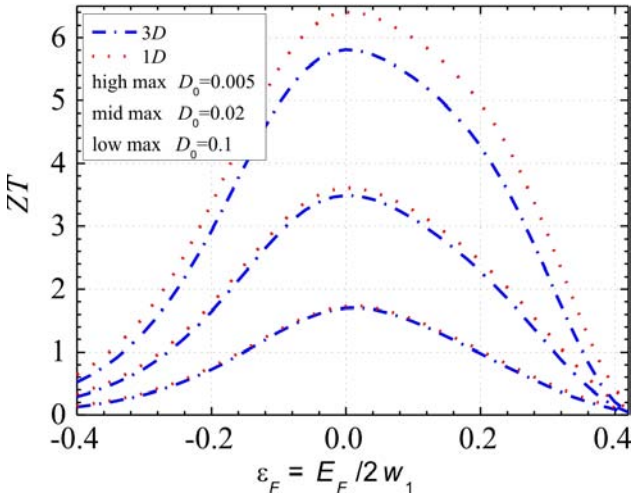

Fig.4. Thermoelectric figure of merit ZT along chains as a function of E_F for $\gamma_1 = 1.7$.

It can be seen that for crystals with $D_0 = 0.1$ and 0.02 the results of 1D and 3D model practically coincide. But for the most perfect crystals ($D_0 = 0.005$) the deviation between the 3D and 1D model becomes important. The decrease of *ZT* in the 3D model with respect to the 1D one achieves 10%, 16% and 40% for $\varepsilon_F = 0$; 0.2 and 0.35, respectively. In stoichiometric crystals (with $\varepsilon_F \sim 0.35$) *ZT* takes very small values even in the most perfect crystals, because the values of the Seebeck coefficient amount to ~ 40 μV/K and thus are very small. In order to increase *ZT* it is therefore necessary to decrease ε_F or the carrier concentration. As it is seen from the Figs. 1-3, in this case the electrical conductivity σ_{xx} decreases, but the thermopower S_{xx} grows considerably and the electronic thermal

conductivity κ_{xx}^{e} decreases. Thus, if ε_F is decreased down to 0.2 (the carrier concentration is decreased by 1.5 times, from $1.2\cdot10^{27}$ m^{-3} down to $0.81\cdot10^{27}$ m^{-3}) *ZT* is expected to achieve values of 1.0 in existing crystals grown by gas phase method with stoichiometric $\sigma_{xx} \sim 10^6$ $\Omega^{-1}m^{-1}$. The predicted thermoelectric parameters in this case are: $\sigma_{xx} = 4.1\cdot10^5$ $\Omega^{-1}m^{-1}$, $S_{xx} = 113$ μV/K, $\kappa_{xx}^{e} = 1.8$ $Wm^{-1}K^{-1}$ and $\kappa_{xx} = 2.4$ $Wm^{-1}K^{-1}$. The main contribution to the increase of *ZT* originates from the increase of the power factor $P_{xx} = \sigma_{xx}S_{xx}^2$. Now for TTT_2I_3 $P_{xx} = 5.2\cdot10^{-3}$ $Wm^{-1}K^{-2}$ which is higher than in Bi_2Te_3, were also $ZT \sim 1$, but $P_{xx} = 4\cdot10^{-3}$ $Wm^{-1}K^{-2}$.

Even higher values of $ZT \sim 2.2$ are expected in more perfect crystals with somewhat higher $\sigma_{xx} \sim 3\cdot10^6$ $\Omega^{-1}m^{-1}$ but which have not been obtained yet. The predicted parameters in this case are: $\sigma_{xx} = 11\cdot10^5$ $\Omega^{-1}m^{-1}$, $S_{xx} = 132$ μV/K, $\kappa_{xx}^{e} = 3.6$ $Wm^{-1}K^{-1}$ and $\kappa_{xx} = 4.2$ $Wm^{-1}K^{-1}$. In this case P_{xx} achieves a value of $1.9\cdot10^{-2}$ $Wm^{-1}K^{-2}$ which is about 4.7 times higher than that of Bi_2Te_3.

In this context, we can conclude that values of $ZT \sim 20$, predicted earlier in highly conducting Q1D organic crystals, are not realizable in TTT_2I_3, because in very pure crystals the carrier mobility becomes limited by the carrier scattering on adjacent chains. It is possible that in other structures, composed of more independent highly conducting molecular chains, such high values of *ZT* could be realized. But values of $ZT \sim 4$ are predicted in still more perfect crystals of TTT_2I_3 with stoichiometric $\sigma_{xx} \sim 6.6\cdot10^6$ $\Omega^{-1}m^{-1}$, if ε_F is decreased up to 0.2. The expected parameters in this case are: $\sigma_{xx} = 2.1\cdot10^6$ $\Omega^{-1}m^{-1}$, $S_{xx} = 146$ μV/K, $\kappa_{xx}^{e} = 5.2$ $Wm^{-1}K^{-1}$ and $\kappa_{xx} = 5.8$ $Wm^{-1}K^{-1}$. The thermal conductivity is increased considerably by 3.5 times with respect to Bi_2Te_3, but now the power factor amounts to $P_{xx} = 4.4\cdot10^{-2}$ $Wm^{-1}K^{-2}$, which is about 11 times higher than in Bi_2Te_3. Thus, if the crystals are more perfect, still more contribution to the increase of *ZT* comes from the increase of the power factor. This is favorable for the thermoelectric applications, because *ZT* is not limited by the lowest value of lattice thermal conductivity.

Conclusions

Detailed modeling of the thermoelectric properties of highly conducting quasi-one dimensional (Q1D) charge transfer organic crystals of TTT_2I_3 in the most comprehensive 3D physical model are presented. These crystals have the advantages that the density of electronic states is increased due to the low dimensionality of the carrier spectrum and the interdependence between electrical conductivity, thermopower and electronic thermal conductivity is somewhat compensated by the more diverse internal interactions. The dependences of electrical conductivity σ_{xx}, thermopower S_{xx}, electronic thermal conductivity κ_{xx}^{e} and of the thermoelectric figure of merit *ZT* along the chains on Fermi energy at room temperature are presented for 1D and 3D physical models. Three sets of TTT_2I_3 crystals are considered: rather pure ones with stoichiometric electrical conductivity $\sigma_{xx} \sim 10^6$ $\Omega^{-1}m^{-1}$, grown previously by the gas phase method [37], more perfect crystals with somewhat higher $\sigma_{xx} \sim 3\cdot10^6$ $\Omega^{-1}m^{-1}$, and even more perfect ones with $\sigma_{xx} \sim 6.6\cdot10^6$ $\Omega^{-1}m^{-1}$, not synthesized yet. It is shown that for the first and second set of samples the results of 1D and 3D model practically coincide. For the third set the scattering on adjacent chains becomes important and it is necessary to apply the 3D model to correctly describe the thermoelectric characteristics. It is obtained that in stoichiometric crystals *ZT* takes very small values even in the most perfect crystals, because the values of the Seebeck coefficient are about ~ 40 μV/K and thus are only very small. In order to increase *ZT* it is necessary to decrease the Fermi energy or the carrier concentration. Thus, if the carrier concentration is decreased

by 1.5 times, from $1.2 \cdot 10^{27}$ m^{-3} down to $0.81 \cdot 10^{27}$ m^{-3}, it is expected to obtain ZT = 1.0 in existing crystals with stoichiometric $\sigma_{xx} \sim 10^6$ $\Omega^{-1}m^{-1}$. Higher values of $ZT \sim 2.2$ are expected in more perfect crystals with somewhat higher $\sigma_{xx} \sim 3 \cdot 10^6$ $\Omega^{-1}m^{-1}$ but have not been obtained yet, and even $ZT \sim 4$ in still more perfect crystals of TTT_2I_3 with stoichiometric $\sigma_{xx} \sim 6.6 \cdot 10^6$ $\Omega^{-1}m^{-1}$. It is important to note that although the electronic part of the thermal conductivity grows considerably with increase of σ_{xx}, the main contribution to the increase of ZT originates from the increase of the power factor which is by 1.3; 4.7 and 11 times higher than that in Bi_2Te_3, respectively for three ZT values mentioned. With the decrease of carrier concentration the thermopower grows considerably and the rise is even bigger in the most perfect crystals. The optimal thermoelectric parameters which would permit to obtain the above mentioned values of ZT are determined.

Acknowledgement The authors gratefully acknowledge the support from EU Commission FP7 program under the grant no. 308768.

References

1. D. Bilc, S.D. Mahanti, E. Quarez, K-F. Hsu, R. Pcionek, and M.G. Kanatzidis, Resonant States in Electronic Structures of the High Performance $AgPb_mSbTe_{2+m}$: The Role of *Ag-Sb* Microstructures, *Phys. Rev. Lett.* **93**, 146403-1 (2004).
2. R. Venkatasubramanian, E. Sivola, et al. Thin-film Thermoelectric Devices with High Room-Temperature Figure of Merit, *Nature* **413**, 597 (2001).
3. M.S. Dresselhaus and J.P.Heremans in: *Thermoelectric Handbook, Macro to Nano*, Ed. by D. M. Rowe, CRC Press, 2006, Chap. 39 (and references therein).
4. C.B. Vining, *ZT*~ 3.5: Fifteen Years Progress and Things to Come, *Proc. of 5th Europe Conf. on Thermoel.* (Odessa. 2007), p. 5-10.
5. T.C. Harman, M.P. Walsh, B.E. LaForge, and G.W. Turner, Nanostructured Thermoelectric Materials. *J. Electronic Mater*. **34**, L19-L22 (2005).
6. Marlow Inc., "Transmission Lasers (DWDM)", as accessed on the website: http://www.marlow.com/industries/telecommunications/transmission-lasers-dwdm.html.
7. Gentherm, "Climate Seats", as accessed on the website: http://www.gentherm.com/page/climate-seats.
8. "Koolatron", as accessed on the website: http://www.koolatron.com/
9. G-H. Kim, L. Shao, K. Zhang, and K. P. Pipe, Engineered Doping of Organic Semiconductors for Enhanced Thermoelectric Efficiency, *Nat. Mater*. **12**, 719 (2013), DOI: 10.1038/NMAT3635.
10. T. Park, C. Park, B. Kim, H. Shin, and H. Kim, Flexible PEDOT Electrodes with Large Thermoelectric Power Factors to Generate Electricity by the Touch of Fingertips, *Energy Environ. Sci.* **6**, 788 (2013).
11. Y. M. Sun, P. Sheng, C. A. Di, F. Jiao, W. Xu, D. Qiu, and D. Zhu, Organic Thermoelectric Materials and Devices Based on *p* - and *n* -Type Poly(metal 1,1,2,2-ethenetetrathiolate)s, *Adv. Mater*. **24**, 932 (2012).
12. N. E. Coates, S. K. Yee, B. McCulloch, K. C. See, A. Majumdar, R. A. Segalman, and Jeffrey J. Urban, *Adv. Mater*. 25 , 1629 (2013).
13. W.Q.Ao, L.Wang, J. Q. Li, F.Pan, and C.N.Wu, Synthesis and Characterization of Polythiophene/Bi2Te3 Nanocomposite Thermoelectric Material, *J.Electron. Mat*. **40,** 9 (2011).
14. N. Toshima, N. Jiravanichanun, and H. Marutani, Organic Thermoelectric Materials Composed of Conducting Polymers and Metal Particles. *J. Electron. Mat*. **41**, 6 (2012).

15. J. Carrete, N. Mingo, G. Tian, H. Agren, A. Baev, and P. N. Prasad, Thermoelectric Properties of Hybrid Organic–Inorganic Superlattices, *The Journal of Physical Chemistry* C **116** (20), 10881 (2012).
16. Jihui Yang, Hin-Lap Yip, and Alex K.-Y. Jen, Rational Design of Advanced Thermoelectric Materials, *Advanced Energy Materials* **3**, 549 (2013).
17. P.J. Troni, I. Hoces, I. Singelin N.et al. Thermoelectric Materials: A Brief Historical Survey from Metal Junctions and Inorganic Semiconductors to Organic Polymers, *Isr. J. Chem*. **54**, 534-552 (2014).
18. Shane P. Ashby, Jorge García-Cañadas, Gao Min and Yimin Chao, *JEM*, **42**, 1495 (2013).
19. G. Kim, K. P. Pipe, Thermoelectric Model to Characterize Carrier Transport in Organic Semiconductors. *Phys. Rev.* ***B***, **86**, 085208 (2012).
20. J. Chen, D. Wang, Z. Shuai, First-Principles Predictions of Thermoelectric Figure of Merit for Organic Materials: Deformation Potential Approximation. *J. Chem. Theory Comput*. **8** (9), 3338 (2012) DOI: 10.1021/ct3004436.
21. J. Yang, Hin-Lap Yip, and Alex K.-Y. Jen, Rational Design of Advanced Thermoelectric Materials, *Advanced Energy Materials* **3**, 5, 549–565 (2013).
22. D. Wang et al., Modeling Thermoelectric Transport in Organic Materials, *Phys. Chem. Chem. Phys.***14**, 16505-16520 (2012), DOI: 10.1039/C2CP42710A
23. W. Shi, J. Chen, J. Hi et al., Search for Organic Thermoelectric Materials with High Mobility: The Case of 2,7-Dialkyl[1]benzothieno[3,2-b][1]benzothiophene Derivatives, *Chem. Mater*. **26**, 669−2677 (2014).
24. Y. Wang, J. Zhou, and R. Yang. *J. Phys. Chem. C* **115**, 24418 (2011).
25. A. Casian in: *Thermoelectric Handbook, Macro to Nano*, Ed. by D. M. Rowe, CRC Press, 2006, Chap.36.
26. A. Casian, Prospects of the Thermoelectricity Based on Organic Materials, *J. Thermoelectricity* **3**, 45 (2007).
27. V.F. Kaminskii, M.L. Khidekel', R.B. Lyubovskii et all. *Phys. Status Solidi* A **44**, 77 (1977).
28. A. Casian, I. Sanduleac, Thermoelectric Properties of Tetrathiotetracene Iodide Crystals: Modeling and Experiment, *J. Electron. Mat*. **43**, 3740 (2014).
29. A. Casian, I. Sanduleac, Effect of Interchain Interaction on Electrical Conductivity in Quasi-One-Dimensional Organic Crystals of Tetrathiotetracene-Iodide, *J. Nanoelectronics and Optoelectronics* **7**, 706-711 (2012).
30. A. I. Casian, I. I. Sanduleac, Organic Thermoelectric Materials: New Opportunities, *J.Thermoelectricity*, **3**, 2013.
31. I. I. Sanduleac, A. I. Casian, J. Pflaum, Thermoelectric Properties of Nanostructured Tetrathiotetracene Iodide Crystals in a Two-Dimensional Model, *Journal of Nanoelectronics and Optoelectronics*, **9**, 247-252, 2014.
32. I. I. Sanduleac, Thermoelectric Power Factor of TTT_2I_3 Quasi-One-Dimensional Crystals in the 3D Physical Model, *J. Thermoelectricity* **4**, 50 (2014).
33. A. Casian, I. Sanduleac, Thermoelectric Properties of Nanostructured Tetrathiotetracene Iodide Crystals: 3D Modeling, *Mat. Today Proc*. (2015), in press.
34. A. Casian, V. Dusciac, and Iu. Coropceanu. Huge Carrier Mobilities Expected in Quasi-One-Dimensional Organic Crystals. *Phys. Rev.* ***B*** **66**, 165404 (2002).
35. A. Casian, V. Dusciac, and V. Nicic. Thermoelectric Opportunities of Quasi-One-Dimensional Organic Crystals of Tetrathiotetracene–Iodide, *J. Thermoelectricity* **2**, 33-39 (2009).

36. A. Casian, J. Stockholm, V. Dusciac, and V. Nicik, Low-Dimensional Organic Crystal Tetrathiotetracene–Iodide as Thermoelectric Material: Reality and Prospects, *J. Nanoelectronics and Optoelectronics* **4**, 95-100 (2009).
37. B. Hilti and C.W. Mayer, Electrical Properties of the Organic Metallic Compound bis (Tetrathiotetracene)-Triiodide, $(TTT)_2I_3$, *Helvetica Chimica Acta* **61** (40), 501(1978).

Submitted 25.02.2015